FOLIA HISTOCHEMICA ET CYTOBIOLOGICA
Vol. 61, No. 3, 2023
pp. 160–171

ORIGINAL PAPER

VIA MEDICA

Therapeutic effect of exosomes derived from hepatocyte-growth-factor-overexpressing adipose mesenchymal stem cells on liver injury

Liushenyan Yu, Junchao Xue, Yanyan Wu, Hanyu Zhou

Department of Pharmacy, Tongde Hospital of Zhejiang province, 310012 Hangzhou, Zhejiang, China

Abstract

Introduction. Adipose mesenchymal stem cell-derived exosomes (ADMSC-Exo) are a new strategy for the treatment of liver injury. However, mesenchymal stem cells (MSCs) exert therapeutic effects mainly by secreting hepatocyte growth factor (HGF). Therefore, we investigated the role of exosomes derived from ADMSC that overexpress HGF ($ADMSC^{HGF}$-Exo) on liver injury.

Material and methods. ADMSCs were isolated from young BALB/c female mice. Then exosomes derived from ADMSC transfecting negative control ($ADMSC^{NC}$-Exo) and HGF overexpression ($ADMSC^{HGF}$-Exo) were isolated and identified by quantitative polymerase chain reaction (qPCR), flow cytometry, western blot, transmission electron microscope and Nanosight particle tracking analysis. These exosomes were injected into male mice *via* tail vein after inducing liver injury by administering 40% carbon tetrachloride (CCl_4)-olive oil twice a week (3 mL/kg, subcutaneously) for 6 weeks. Liver injury and liver collagen fiber accumulation were determined by histopathological analysis. Then, the levels of serum liver function indexes (alanine aminotransferase, aspartate aminotransferase, albumin, total bilirubin), hepatocyte-specific markers (albumin, cytokeratin-18 and hepatocyte nuclear factor 4α), hepatic fibrosis-related proteins (α-smooth muscle actin and collagen I) and Rho GTPase (cell division cycle 42 and ras-related C3 botulinum toxin substrate 1) were determined by Enzyme-linked immunosorbent assay (ELISA), immunohistochemistry, Western blot and qPCR.

Results. ADMSCs were identified by high expression of CD105 and CD44 molecules and low expression of CD45 and CD34. ADMSCs-Exo, $ADMSC^{NC}$-Exo and $ADMSC^{HGF}$-Exo transfected cells had similar expression of exosome-specific membrane proteins (CD63, CD81 and CD9). Mice with CCl_4-induced liver injury exhibited abnormal serum liver function indexes, altered expression of hepatocyte-specific markers, hepatic fibrosis-related proteins and Rho GTPase protein as well as histopathological changes and collagen fiber accumulation in the liver. These changes were reversed by ADMSC-Exo, $ADMSC^{NC}$-Exo and $ADMSC^{HGF}$-Exo administration with $ADMSC^{HGF}$-Exo displaying the most significant impact.

Conclusions. $ADMSC^{HGF}$-Exo exerted a hepatoprotective effect in mice with experimental liver injury by alleviating hepatic fibrosis and restoring liver function. *(Folia Histochemica et Cytobiologica 2023, Vol. 61, No. 3, 160–171)*

Keywords: liver injury; adipose mesenchymal stem cells; Hepatocyte growth factor; exosome; Rho GTPase

Introduction

The liver is vital for many important body functions, such as protein synthesis, anti-virus and anti-bacteria [1]. In addition, the liver also is the major detoxification organ, which is most exposed to drugs, chemicals and alcohol. Long-term exposure to excessive hazardous substances will lead to liver injury, ultimately impacting patients' health conditions and life quality [2]. Although some drugs, such as N-acetylcysteine, are approved for the treatment of liver injury, they have limited efficacy and significant side effects [3]. Therefore, it is urgent to find more safe and effective drugs for alleviating liver injury.

Correspondence address:
Hanyu Zhou
Department of Pharmacy, Tongde Hospital of Zhejiang province, No. 234 Gucui Road, Xihu District, 310012 Hangzhou, Zhejiang, China
e-mail: elainehanyu@163.com

Folia Histochem Cytobiol. 2023
10.5603/fhc.95291
ISSN 0239-8508, e-ISSN 1897-5631

www.journals.viamedica.pl/folia_histochemica_cytobiologica

The accumulated research indicated that mesenchymal stem cells (MSCs) have great potential in promoting liver regeneration and liver injury repair [4]. MSCs come from a wide range of sources, including adipose [5], bone marrow [6] and synovial tissues [7]. Of note, compared with other MSCs, adipose-derived MSCs (ADMSCs) are plentiful and can be easily obtained without severe invasiveness and ethical issues [8, 9]. Notably, recent studies have shown that ADMSCs have achieved certain therapeutic effects in some diseases by secreting exosomes [10–12]. Exosomes with a diameter of 40–100 nm can be secreted by donor cells and then delivered to recipient cells, thus playing a role in cell-to-cell communication [13–15]. It is well known that exosomes released by ADMSCs play a functional role in diseases by mimicking the effects of their parental cells, thus, we hypothesized that exosomes derived from ADMSCs may become a potential therapy for liver injury [16].

Hepatocyte growth factor (HGF) is a growth factor secreted by various cell types including MSCs [17], which exerts an important effect in promoting liver regeneration and repairing liver injury [18]. Multiple studies have shown that the overexpression of HGF can prevent acute liver injury induced by oxidative stress [19] and carbon tetrachloride (CCl_4) [20], alleviate liver fibrosis [21], and accelerate liver regeneration in injured liver injury [22]. Interestingly, Cao *et al.* reported that the exosomes derived from ADMSCs that overexpressed HGF ($ADMSC^{HGF}$-Exo) were more capable of skin wound repair in diabetic mice than the exosomes derived from control ADMSCs ($ADMSC^{NC}$-Exo) [23]. However, it is not clear which role $ADMSC^{HGF}$-Exo can play in liver injury. Studies have shown that proteins of Rho GTPase family are associated with the development of liver fibrosis [24], non-alcoholic fatty liver degeneration [25] and liver cancer [26]. Interestingly, HGF can regulate Rho GTPase in prostate cancer cells [27]. However, it is not clear whether $ADMSC^{HGF}$-Exo can influence the development of liver injury by affecting Rho GTPase.

Therefore, in this study, we used an established model of murine liver injury to verify the potential therapeutic effects of $ADMSC^{HGF}$-Exo.

Material and methods

Animals and experimental design. Specific pathogen-free BALB/c female mice (n = 5, 8–10 g, 3 weeks old) and BALB/c male mice (n = 30, 6 per group, 18–25 g, 6–8 weeks old) obtained from Shanghai Slake Animal Laboratory Co. Ltd (Certificate No. SCXK (Hu) 2017-0005) were maintained in an environment (22 ± 2°C) with a 12 h:12 h light-dark cycle and 50% humidity. BALB/c female mice were used to isolate ADMSCs, while BALB/c male mice were used to construct liver injury models.

The isolation and identification of ADMSCs. After the mice were euthanized with an overdose of isoflurane (5%), the subcutaneous adipose tissues in the medial inguinal region of the mice were collected and digested in Minimum Essential Medium-alpha (1061029, Gibco, USA) containing 0.1% collagenase type I solution (C1696, Bioswamp, China) at 37°C for 50 min. After centrifugation at 1000 rpm for 5 min, the fat and supernatant from the upper layers were discarded and the cells were re-suspended in Dulbecco's Modified Eagle's Medium/ /Nutrient Mixture F-12 (DMEM/F12) culture medium (ZQ-600, Zqxzbio, China) with the addition of 10% fetal bovine serum (FBS, ZQ500-A, Zqxzbio, China) and 1% penicillin-streptomycin (0513, ZQ500-A, Zqxzbio). Afterward, the cells were centrifuged again at 1000 rpm for 5 min, re-suspended in phosphate-buffered saline (PBS, SNB-001, Sunncell, China), and centrifuged once more at 1000 rpm for 5 min. Finally, the obtained cells were inoculated in DMEM/F12 medium containing 10% FBS at a density of 2×10^5/mL. The medium was changed for the first time after 24 h and every 3 days thereafter. The cells were passaged when they reached 90% confluence, and the morphology of cells of different generations was observed under an inverted microscope (NIB910, Boshida, China).

The third-generation ADMSCs were identified by flow cytometry (CytoFLEX LX, Beckman Coulter, UK). At first, cells were collected and adjusted to the concentration of 1×10^6/mL, and then identified by the monoclonal antibodies (BD Biosciences, USA): CD45 (560695), CD44 (553134), CD105 (562759) and CD34 (551387) at the dilution of 1:50.

Cell transfection. Genechem Co., Ltd. (China) provided a lentiviral vector (GOSL49905) that overexpressed HGF and a blank lentiviral vector (negative control, NC) that only encoded green fluorescent protein (GFP). Then, we entrusted Genscript Co., Ltd. to package and concentrate lentiviruses. ADMSCs were seeded into 24-well plates at 1×10^5/well 24 h prior to transfection. On that next day, the cell culture medium was replaced with fresh medium containing 6 μg/mL of polybrene (A1001-9, Zqxzbio, China) and 10-fold serially diluted viral suspension. After the cells were incubated at 37°C for 24 h, the medium was changed and the culture was continued for 48 h. The efficiency of GFP expression was observed by fluorescence microscopy (Ts2-FC microscope, Nikon, Tokyo, Japan), and a fresh complete medium containing 1 μg/mL of puromycin was replaced to screen stable transfection cells.

Gene expression analysis. Quantitative polymerase chain reaction (qPCR) was performed to evaluate the transfection efficiency or gene expression. Trizol reagent (ZC-0021, Zcbio, China) was used to extract total RNA from ADMSCs, and RNA purity was assessed by NanodropTM 2000 (ThermoFisher Scientific, Las Vegas, NV, USA). Afterwards, with the use of a reverse transcription kit (AC14007, ACMEC, China), we converted the total RNA to cDNA according to the manufacturer's instructions. Later, qPCR was carried out on an Mx3000P

system (Stratagene, San Diego, CA, USA) employing SYBR Green PCR Mastermix (ac17097, ACMEC, China). The cycle parameters for qPCR were as followed: pre-denaturation at 95°C for 10 min, denaturation at 95°C for 15 s, and annealing at 60°C for 60 s for 40 cycles. β-actin was considered as a housekeeping gene, and $2^{-\Delta\Delta CT}$ method was used as previously described with minor modifications to detect the mRNA expression of HGF, Albumin (ALB), Cytokeratin-18 (CK-18), hepatocyte nuclear factor 4α (HNF4α), α-smooth muscle actin (α-SMA), Collagen I, cell division cycle 42 (CDC42), ras-related C3 botulinum toxin substrate 1 (Rac1) [28]. Primers that were used in our experiment were listed as followed:

- HGF (mouse) forward, 5'-GGTTACAGGGGA-ACCAGCAA -3'
- HGF (mouse) reverse, 5'-TCGGATGTTTGGG-TCAGTGG-3'
- ALB (mouse) forward, 5'-GTGGATCCCTGG-TGGAAAGG-3'
- ALB (mouse) reverse, 5'-GGTTTGGACCCT-CAGTCGAG-3'
- CK-18 (mouse) forward, 5'-GACATCCATG-GACTCCGCAA-3'
- CK-18 (mouse) reverse, 5'-ATCTGTGCCTTG-TATCGGGC-3'
- HNF4α (mouse) forward, 5'-GGGGTTCTGC-TGGCTCATAC-3'
- HNF4α (mouse) reverse, 5'-GATGCTTTCC-CAATGACGGC-3'
- α-SMA (mouse) forward, 5'-GAATGCAGTG-GAAGAGACCCA-3'
- α-SMA (mouse) reverse, 5'-GCAGGGCATA-GCCCTCATAG-3'
- Collagen I (mouse) forward, 5'-GAGCGGA-GAGTACTGGATCG-3'
- Collagen I (mouse) reverse, 5'-GCTTCTTT-TCCTTGGGGTTC-3'
- CDC42 (mouse) forward, 5'-CCTCCGGAAAC-TCAACCCAA-3'
- CDC42 (mouse) reverse, 5'-CTAGCAAGCCA-ACCCTTTTCA-3'
- Rac1 (mouse) forward, 5'-TGTCCCCCTCC-TGTCAAGAA-3'
- Rac1 (mouse) reverse, 5'-GCATCAAATGCGA-AGGCTCG-3'
- β-actin forward, 5'-GGGAAATCGTGCGTGAC -3'
- β-actin reverse, 5'-AGGCTGGAAAAGAGCCT -3'

Isolation and identification of exosomes from ADMSCs. The exosomes were obtained using an exosome isolation kit (41201ES25, Yeasen, China). The culture medium of ADMSCs was collected into a 15 mL centrifuge tube and centrifuged at 3000 *g* for 10 min. The supernatant (10 mL) from the centrifuge tube was transferred to a new centrifuge tube, which was mixed with an exosome separation reagent (2.5 mL) and placed at 4°C for 2 h. The mixture was centrifuged at 10,000 *g* for 60 min and the precipitate was collected and resuspended in 100 μL PBS. The samples were centrifuged at 12000 *g* for 2 min to obtain the supernatant. Then the supernatant was filtrated with a 0.22 μm filter to purify the exosomes.

The morphology of exosomes was observed under a transmission electron microscope (TEM, H7650, Hitachi, Japan) at the Medical Research Center, Academy of Chinese Medical Sciences (Zhejiang, China). In short, approximately 25 μL of exosome sample was dropped on a carbon-coated grid. After 2 min, the grid was incubated again with 2% phosphotungstic acid for 2 min, and its edges were dried with filter paper. Finally, images were obtained by TEM. Moreover, exosome diameter was analyzed with nanoparticle tracking analysis (NTA, Nano-Sight NS300, Malvern Instruments, UK). Exosome surface markers (CD63, CD81 and CD9) were detected using Western blot.

Western blot. The total protein in mouse liver tissues and exosome protein in ADMSCs-Exo, $ADMSC^{NC}$-Exo and $ADMSC^{HGF}$-Exo were extracted by RIPA solution (AC13971, Acmec, China) and exosome protein extraction kit (BES21253BO, Bioesn, China), respectively. Afterwards, the concentration of protein was determined by the bicinchoninic acid (BCA) assay kit (AC13859, Acmec, China). Sodium dodecyl sulfate polyacrylamide (SDS-PAGE) gels gel electrophoresis was performed to separate proteins, after which the proteins were loaded onto the Polyvinylidene Fluoride (PVDF) membranes (0.2 μm, FFP24, Beyotime, China). After being blocked with a blocking buffer (ZY100878, Zeye Biotechnology, China), the membranes were incubated with specific primary antibodies for 24 h. In the following, the complex on the membrane was bound by the secondary antibody. Finally, the protein bands were exposed using imaging equipment (610020-9Q, Qinxinag, China) outfitted with an enhanced chemiluminescence kit (P1020-100, APPLYGEN, China).

The information of the primary antibodies was as follows: CD63 (AF5117, 26 kDa), CD81 (DF2306, 26 kDa), CD9 (AF5139, 25 kDa), ALB (DF6396, 69 kDa), CK-18 (AF0191, 48 kDa), HNF4α (AF6297, 53 kDa), α-SMA (AF1032, 42 kDa), Collagen-I (AF7001, 129 kDa), CDC42 (ab187643, 1/10000, 21 kDa), Rac1 (ab155938, 21 kDa) and β-actin (AF7018, 1/10000, 42 kDa). Unless otherwise specified, the dilution of other antibodies was 1/1000. All of the antibodies were obtained from Abcam (Waltham, MA, USA) or Affinity (USA).

Establishment of liver injury model. Liver injury mice were established as previously described with minor modifications [29–31]. BALB/c male mice were randomized into 5 groups: control group, model group, ADMSC-Exo group, $ADMSC^{NC}$-Exo group and $ADMSC^{HGF}$-Exo group (n = 6). In the latter four groups, mice were subcutaneously (*s.c.*) injected with 40% CCl_4-olive oil solution 5 mL/kg on the first day. Then, mice were subcutaneously injected with 40% CCl_4-olive oil (3 mL/kg) twice a week for 6 weeks. At the same time, these

Folia Histochem Cytobiol. 2023
10.5603/fhc.95291
ISSN 0239-8508, e-ISSN 1897-5631

mice were fed with high-fat and low-protein feed (79.5% pure corn flour and 20% lard, mixed with 0.5% cholesterol) and 0.5% alcohol was added to drinking water. The mice in the control group were injected *s.c.* with an equal volume of olive oil solution every time and fed with normal feed and normal drinking water. Blood was taken from orbit sinus and serum was used to measure biochemical indices of liver function. Then, the exosomes isolated from ADMSCs, ADMSCs transfected with NC and ADMSCs overexpressed with HGF (400 μg/μL, 200 μL) were injected into mice *via* tail vein once a week for 4 weeks (during the 4 weeks, mice did not receive CCl_4-olive oil, and were supplied with standard chow diet and normal drinking water). The control mice were injected with the same volume of PBS.

Enzyme-linked immunosorbent assay (ELISA). After mice were treated with ADMSCs for 2 weeks or 4 weeks, their blood was collected from the abdominal aorta and centrifuged to obtain serum. The activities of serum alanine aminotransferase (ALT, ZC-38191), aspartate aminotransferase (AST, ZC-38728), ALB (ZC-37920) and the contents of total bilirubin (TBIL, ZC-38083) in mice were determined by corresponding ELISA kit (Zcibio, China). To extract supernatant serum, mouse blood was collected and centrifuged at 3500 rpm for 15 min. In a well plate, the target antibody was coated first. A serum or a standard was then introduced to the well to bind to the target antibody. After that, a horseradish peroxidase-labeled antibody was added to the well. The 3,3′,5,5′-tetramethylbenzidine (TMB) substrate was added for coloring after the unbound antibody had been thoroughly washed. Finally, a microplate reader (HBS-ScanX, DeTiebio, China) was employed to measure the absorbance at 450 nm.

Hematoxylin and eosin (H&E) staining. The liver samples were fixed in 4% paraformaldehyde (P35120, Acmec, China), then embedded in paraffin and cut with microtome into 4 μm-thick sections. Paraffin slices were dewaxed by xylene, soaked in absolute ethanol, 90% ethanol and 75% ethanol in turn, and finally washed with tap water. The sections were sequentially immersed in hematoxylin dye solution (PAB180015, Bioswamp), shortly washed with tap water, and placed in eosin dye solution (PAB180016, Bioswamp). Subsequently, the sections were successively dehydrated with 70%, 80%, 95% and 100% ethanol, cleared with xylene and finally mounted with neutral balsam (I1711, Bioswamp). The stained sections were observed under an optical microscope (E100, Nikon, Japan).

Sirius red staining. The liver sections were stained with Sirius red staining kits (MM1004, Maokangbio, China) for 1 h. After washing off the surface dyeing solution with tap water, the sections were subjected to conventional dehydration, transparency and sealing.

Immunohistochemistry (IHC). The IHC procedure was carried out using the IHC kit (IHC200) provided by Bioswamp. The treated sections were placed in 0.01M sodium citrate buffer and the antigen was retrieved under high pressure (125°C, 103 KPa). Following that, the sections were incubated with 3% H_2O_2 for 10 min and 10% goat serum for 1 h. After that, the sections were incubated with anti-ALB (1:300, ab192603,), anti-CK-18 (1:800, ab181597), and anti-HNF4α antibodies (1:400, ab199431) overnight at 4°C. The following day, secondary antibodies (1:5000, AF5131, Abcam, USA), were applied dropwise to the sections and incubated for 20 min at room temperature. The sections were next sequentially stained with 3,3-diaminobenzidine (DAB) developing solution and hematoxylin dye solution. After washing with running water again, the sections were subjected to conventional dehydration, transparency and sealing. All the primary antibodies were purchased from Abcam (China).

Statistical analysis. The quantitative data were expressed as mean ± standard deviation (SD). One-way analysis of variance (ANOVA) with Tukey's test were employed to evaluate the significant differences among multiple groups. Dunnett's T3 test or independent sample T test was used for heterogeneity of variance. Kruskal-Wallis H test was used for the measurement of data that did not conform to normal distribution. Utilizing the software SPSS 19.0, the analysis of these data was conducted, and P-values less than 0.05 were considered statistically significant.

Results

Isolation and identification of exosomes derived from ADMSCs

ADMSCs were isolated from mice and cultured in DMEM/F12 medium. As shown in Fig. 1A, ADMSCs exhibited a fibrous or spindle shape with uniform cell morphology. With the help of flow cytometry, we found that ADMSCs were positive for CD105 and CD44 and negative for CD45 and CD34 (Fig. 1B). The above results demonstrated our successful isolation of ADMSCs. After HGF was overexpressed in ADMSCs, levels of mouse HGF mRNA were elevated in ADMSCs^{HGF}, indicating successful transfection (Fig. 2A, $P < 0.01$). Furthermore, there were no significant differences in the expressions of surface markers (CD45, CD44, CD105 and CD34) between ADMSCs^{NC} and ADMSCs^{HGF} (Fig. 2B). Then, exosomes were isolated from ADMSCs, their morphology was shown in Fig. 2C, and their diameter was approximately 200 nm (Fig. 2D). Notably, there were no significant differences in the expressions of CD63, CD81, and CD9 proteins between the ADMSC-Exo and ADMSC^{NC}-Exo, as well as the ADMSC^{NC}-Exo and ADMSC^{HGF}-Exo (Fig. 2E).

ADMSC^{HGF}-Exo treatment improved liver function indexes in serum for liver injury mice

Firstly, the levels of liver function indexes in the serum of liver injury mice after 2 weeks and 4 weeks of ADMSC^{HGF}-Exo treatment were determined. As shown in Fig. 3, the serum ALT, AST and TBIL levels of model

Folia Histochem Cytobiol. 2023
10.5603/fhc.95291
ISSN 0239-8508, e-ISSN 1897-5631

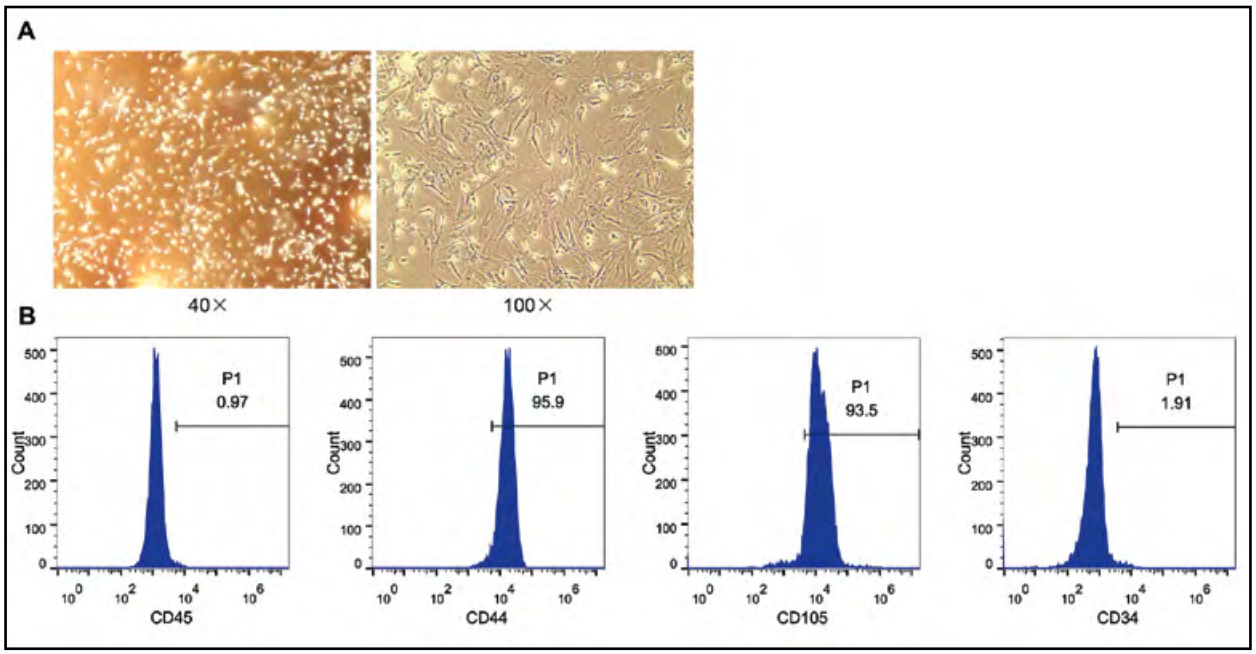

Figure 1. Isolation and identification of ADMSCs. **A.** ADMSCs isolated from mouse subcutaneous fatty tissues were observed under the microscope. **B.** The expressions of ADMSC surface markers, including CD45, CD44, CD105 and CD34 were measured by flow cytometry. n = 3. Abbreviation: ADMSCs — adipose-derived mesenchymal stem cells.

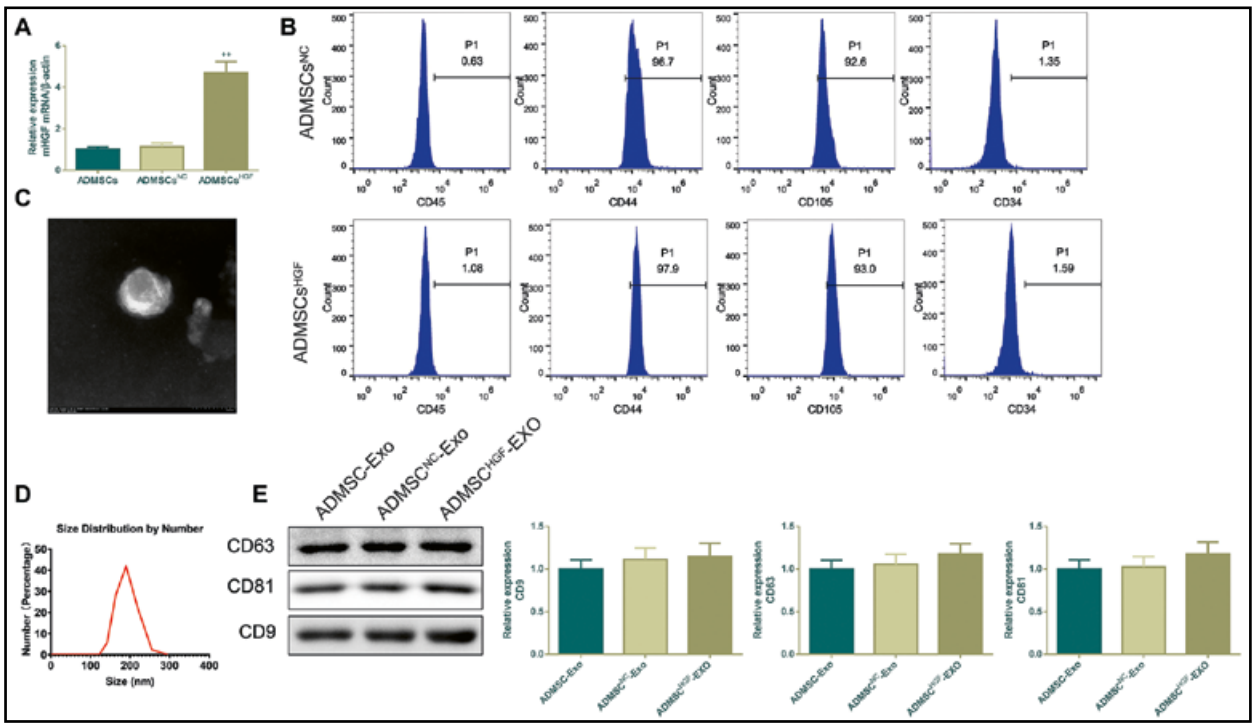

Figure 2. Lentivirus-HGF transfection increased HGF mRNA expression but did not affect the properties of mesenchymal stem cells and Exos. **A.** The expression of HGF mRNA in ADMSCs was detected by qPCR. **B.** Flow cytometry analysis for the expressions of the surface markers of ADMSCs, including CD45, CD44, CD105 and CD34. **C.** The morphology of ADMSC-Exo was viewed by TEM. Scale bar, 100 nm. **D.** Particle size distribution and concentration of ADMSC-Exo were analyzed by NTA. **E.** Detection of ADMSC-Exo marker protein expressions (CD9, CD63, and CD81) by western blot. $^{+}P < 0.05$, and $^{++}P < 0.01$ *vs.* ADMSCs. The results were presented as the mean ± standard deviation. n = 3. Abbreviations: Exo — exosome; HGF — hepatocyte growth factor; NTA — nanoparticle tracking analysis; qPCR — quantitative polymerase chain reaction; TEM — transmission electron microscopy.

Folia Histochem Cytobiol. 2023
10.5603/fhc.95291
ISSN 0239-8508, e-ISSN 1897-5631

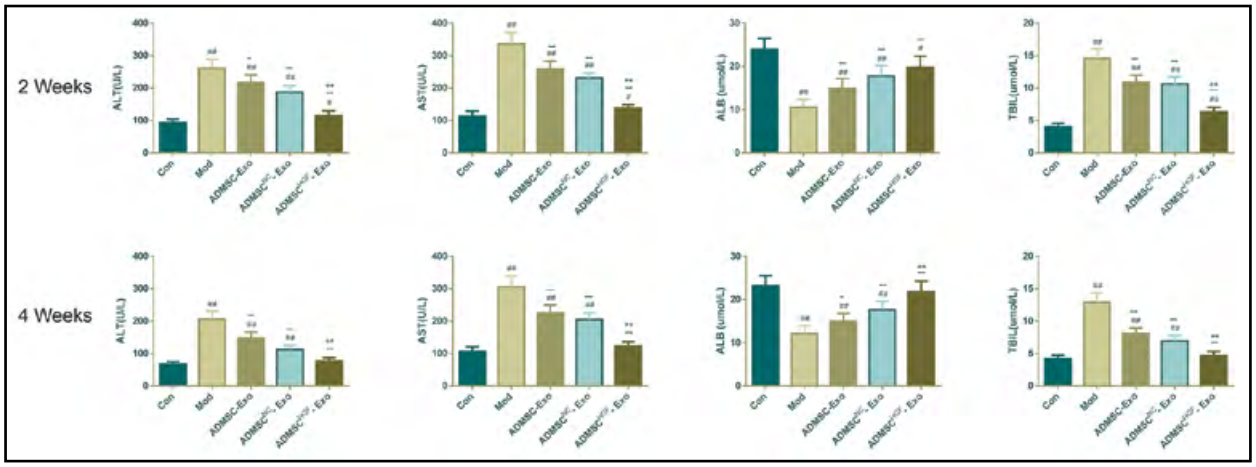

Figure 3. HGF overexpression in ADMSC-Exos improved liver functions of liver injury mice. ELISA was applied to quantify serum ALT and AST activities as well as ALB and TBIL contents of the mice after 2 and 4 weeks of ADMSC treatment. $^{\#}P < 0.05$, and $^{\#\#}P < 0.01$ *vs.*Con; $^{-}P < 0.05$, and $^{--}P < 0.01$ *vs.* Mod; $^{*}P < 0.05$, $^{**}P < 0.01$ *vs.* ADMSC^{NC}-Exo. The results were presented as the mean ± standard deviation. n = 6. Abbreviations: ALB — albumin; ALT — alanine aminotransferase; AST — aspartate aminotransferase; ELISA — Enzyme-linked immunosorbent assay; TBIL — total bilirubin.

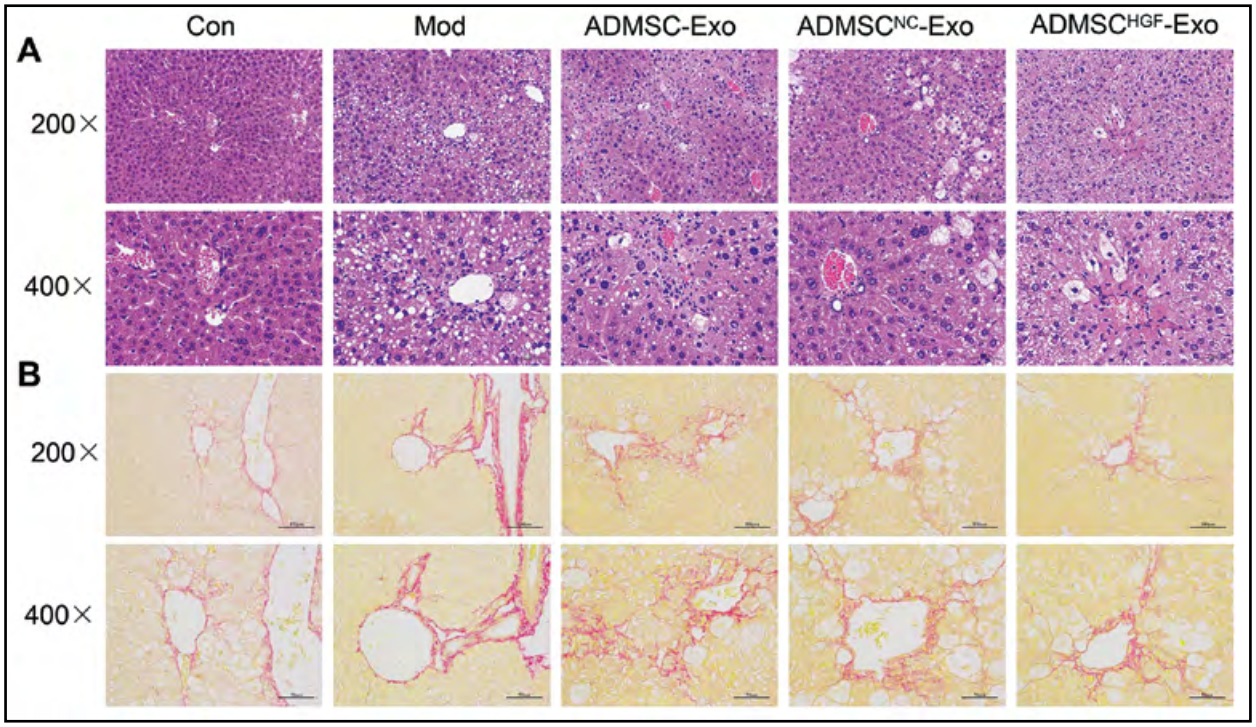

Figure 4. HGF overexpression in ADMSC-Exos recovered the pathological injuries of liver fibrosis in liver injury mice. **A.** The representative images of liver slices stained with HE. **B.** The representative images of liver slices stained by Sirius red. Magnification 200×, scale bar = 100 μm; Magnification 400×, scale bar = 50 μm, n = 6. Abbreviation: HE — hematoxylin and eosin.

mice were significantly higher while the ALB content was significantly lower than these of the control group ($P < 0.01$). However, the exosomes secreted by ADMSCs, NC-transfected ADMSCs or HGF-transfected ADMSCs effectively decreased activities of ALT, AST and TBIL levels but upregulated ALB content in serum of liver-injured mice, among which ADMSC^{HGF}-Exo had the most significant effects ($P < 0.05$).

ADMSC^{HGF}-Exo treatment ameliorated histopathological changes in the liver and hepatic collagen fiber accumulation

The liver samples from mice of experimental groups were collected and the morphology of stained liver sections was analyzed. In the CCl_4-liver injured mice, hepatic lobules were disordered, the structure of liver cells was destroyed, moreover, many necrotic cells and inflammatory cell infiltration were observed in the

Folia Histochem Cytobiol. 2023
10.5603/fhc.95291
ISSN 0239-8508, e-ISSN 1897-5631

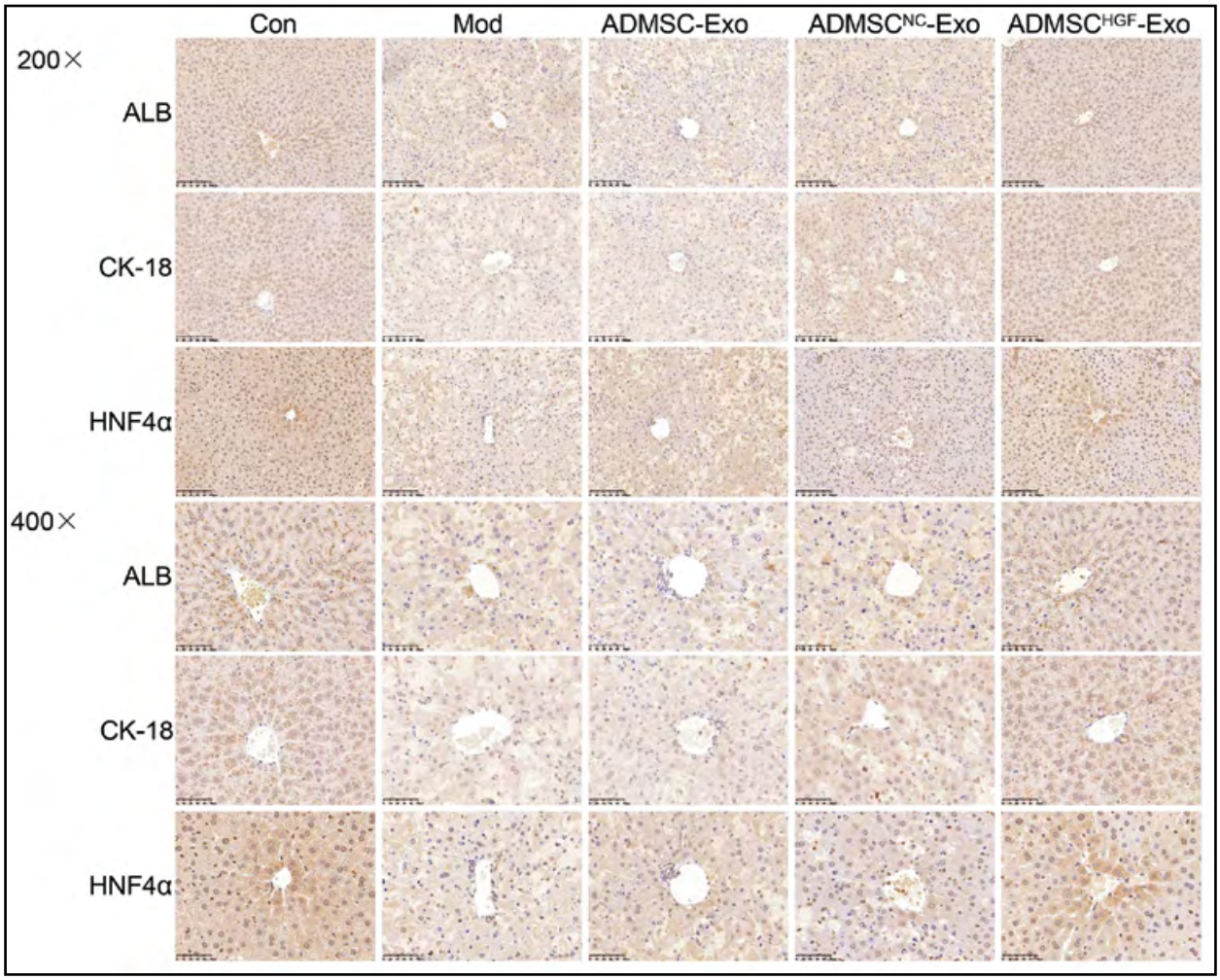

Figure 5. HGF overexpression in ADMSC-Exos promoted hepatic protein expressions in liver injury mice. After 4 weeks of ADMSC treatment, the immunoreactivities of ALB (localized in the cytoplasm), CK-18 (localized in the cytoplasm) and HNF4α (localized in the nucleus) in the liver tissues of the mice were tested by immunohistochemistry. Magnification 200×, scale bar = 100 μm; magnification 400×, scale bar = 50 μm.; n = 6. Abbreviations: CK-18 — Cytokeratin-18; HNF4α — hepatocyte nuclear factor 4α.

liver tissues (Fig. 4A). After treatment with ADMSC--Exo or ADMSC^{NC}-Exo, the histopathological changes of the model mice were alleviated. After treatment of model mice with ADMSC^{HGF}-Exo, the morphology of the liver returned almost to normal with radially arranged hepatocyte cords and sinusoids ending in central veins, however, with some areas of fatty degeneration and necrosis. Moreover, Sirius red staining revealed that the hepatic tissues of the mice in the control group exhibited normal structures (Fig. 4B). However, fiber extension and collagen accumulation which formed partial compartments were observed in the model group, moreover, model mice also developed pseudolobular-like structures in the liver. These lesions were alleviated after the treatment with ADMSC-Exo, ADMSC^{NC}-Exo and ADMSC^{HGF}-Exo, among which ADMSC^{HGF}-Exo had the best effects.

ADMSC^{HGF}-Exo treatment upregulated the expressions of ALB, CK-18 and HNF4α yet downregulated the expression of α-SMA in CCl_4-injured liver

The expressions of hepatocyte markers (ALB, CK-18 and HNF4α) were determined by IHC, qPCR and western blot, and the expression of hepatic fibrosis--related protein (α-SMA) was tested by qPCR and western blot. Firstly, the IHC results unveiled that the immunoreactivities of albumin (localized in the cytoplasm), CK-18 (localized in the cytoplasm) and HNF4α (localized in the nucleus) were downregulated in the CCl_4-damaged liver, while these trends were rescued by ADMSC-Exo, ADMSC^{NC}-Exo and ADMSC^{HGF}-Exo administration, among which ADMSC^{HGF}-EXO had the strongest effect (Fig. 5, $P < 0.01$).

The expressions of hepatocyte markers detected by qPCR and western blot were consistent with the

Folia Histochem Cytobiol. 2023
10.5603/fhc.95291
ISSN 0239-8508, e-ISSN 1897-5631

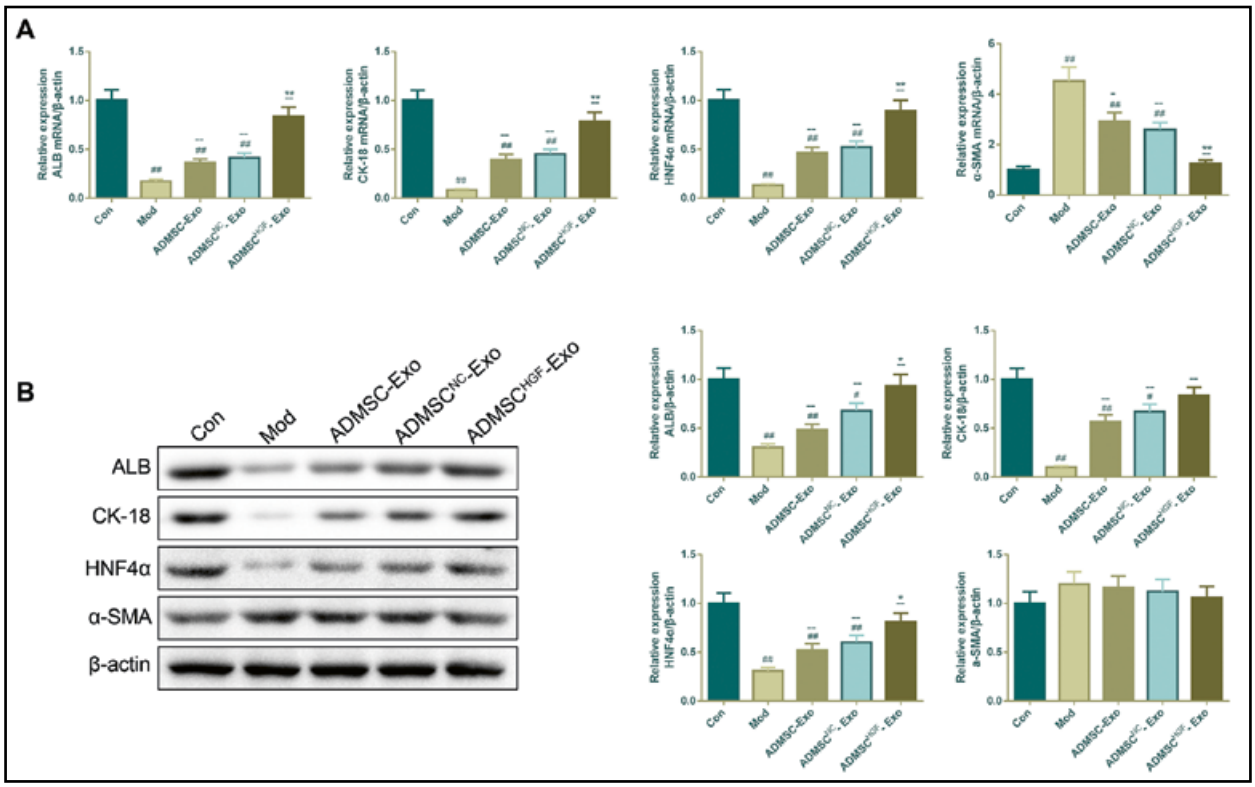

Figure 6. HGF overexpression in ADMSC-Exos facilitated hepatic gene expression but suppressed α-SMA expression in liver injury mice. **A.** After 4 weeks of ADMSC treatment, qPCR was utilized to measure the mRNA levels of ALB, CK-18, HNF4α and α-SMA in the liver tissues of the mice. B. After 4 weeks of ADMSC treatment, western blot was utilized to measure the protein levels of ALB, CK-18, HNF4α and α-SMA in the liver tissues of the mice. The results were presented as the mean ± standard deviation. n = 6. $^{\#}P < 0.05$, and $^{\#\#}P < 0.01$ *vs.* Con; $^{-}P<0.05$, and $^{--}P < 0.01$ *vs.* Mod (model group); $^{*}P < 0.05$, $^{**}P < 0.01$ *vs.* ADMSC^{NC}-Exo. Abbreviation: α-SMA — α-smooth muscle actin.

IHC results (Fig. 6, $P < 0.01$). Specifically, the levels of albumin, CK-18 and HNF4α mRNA and protein expressions were downregulated in CCl_4-liver injured mice, yet, ADMSC-Exo, ADMSCNC-Exo and ADMSCHGF-Exo administration significantly upregulated the levels of albumin, CK-18 and HNF4α mRNA and protein expressions for CCl_4-liver injured mice, among which ADMSC^{HGF}-EXO had the strongest effects ($P < 0.05$). In addition, the upregulation of α-SMA induced by modeling was reversed by ADMSC-Exo, ADMSC^{NC}-Exo and ADMSC^{HGF}-Exo, however, the mRNA level of α-SMA changed significantly ($P < 0.01$) but the protein level did not.

ADMSC^{HGF}-Exo treatment suppressed the expressions of Collagen I and Rho GTPase in liver for liver injury mice

The results of qPCR and western blot revealed that the expressions of Collagen I and Rho GTPase (CDC42 and Rac1) were higher in the model group than in the control group (Fig. 7A, B; $P < 0.01$). However, the overexpressing Collagen I, CDC42 and Rac1 were suppressed by ADMSC-Exo, ADMSC^{NC}-Exo and ADMSC^{HGF}-Exo, among which ADMSC^{HGF}-EXO had the strongest effects ($P < 0.05$).

Discussion

Recently, stem cells and their underlying utilization in cell therapy have drawn much attention, owing to their capacity of self-renewal and differentiation into many cell types in different inducing environments [32]. Utilizing the paracrine mechanism of MSCs is a promising strategy to promote liver regeneration and repair liver injury [33]. Additionally, both human and rat MSCs have the ability to differentiate into hepatocyte-like cells after transplantation into the liver of rats [34]. Clinical trials have also found that MSCs' injection can be utilized to treat liver disorders with satisfying therapeutic effects and high tolerability [35, 36]. In addition, ADMSCs offer numerous advantages over other sources of MSCs in terms of ethical acquisition, origin, renewal characteristics, and immunogenicity [37]. Therefore, we studied the

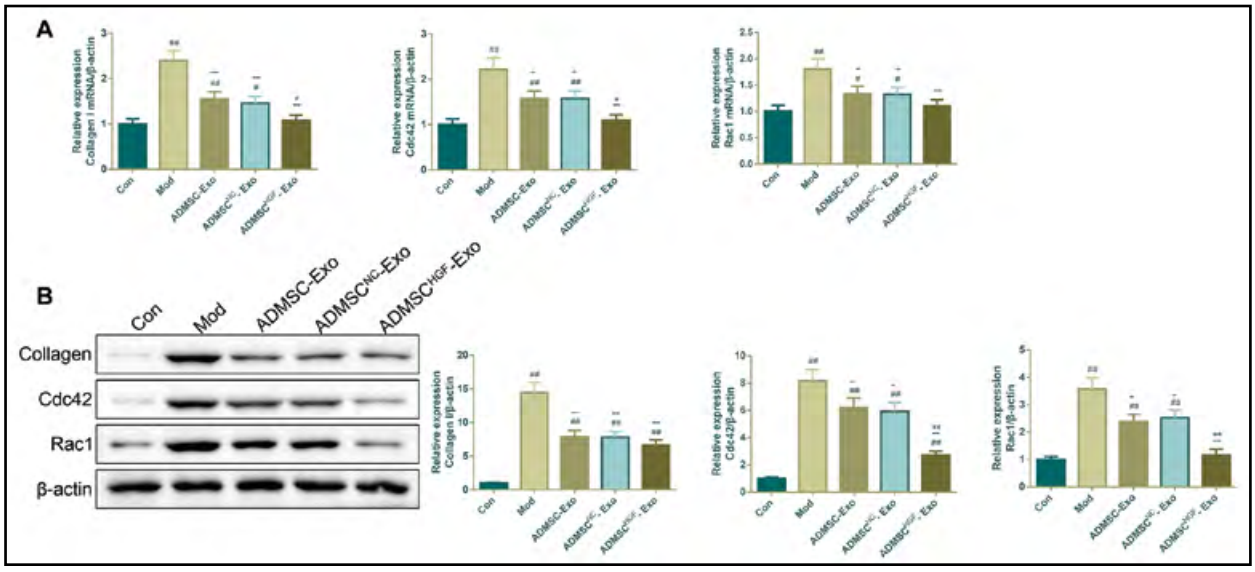

Figure 7. HGF overexpression in ADMSC-Exos ameliorated liver fibrosis in liver injury mice by suppressing the Rho pathway. After 4 weeks of ADMSC treatment, the expressions of Collagen I, CDC42 and Rac1 in the liver tissues of the mice were detected at both mRNA (A) and protein (B) levels. The results were presented as the mean ± standard deviation. n = 6. $^{\#}P < 0.05$, and $^{\#\#}P < 0.01$ *vs.* Con; $^{-}P < 0.05$, and $^{--}P < 0.01$ *vs.* Mod (model group); $^{*}P < 0.05$, $^{**}P < 0.01$ *vs.* ADMSCNC-Exo. Abbreviations: CDC42 — cell division cycle 42; Rac1 — Ras-related C3 botulinum toxin substrate 1.

role of ADMSCs-Exo in liver injury. In this study, we first identified primary cultured ADMSCs. CD105 and CD44 are generally considered markers of MSCs, while CD45 and CD34 are hematopoietic markers. In the previous study, ADMSCs expressed CD105 and CD44, but hardly expressed CD45 and CD34 [38]. Our research was consistent with the previous research, which suggests that we have successfully isolated ADMSCs. Subsequently, we identified the exosomes, and all of them expressed exosome-specific membrane proteins (CD63, CD81 and CD9) [39], which indicated that we successfully isolated exosomes. In addition, ADMSC-Exo, ADMSC^{NC}-Exo and ADMSC^{HGF}-Exo have the same expressions of exosome-specific membrane proteins, which implies that HGF overexpression did not affect exosome secretion.

The CCl_4-induced animal model is a classical model for screening protective drugs against liver injury, and its main mechanism is that CCl_4 activates cytochrome P-450 to form extremely toxic trichloromethyl (CCl_3•) as well as trichloromethyl peroxyl (CCl_3O_2•) free radicals [40]. Then, both CCl_3• as well as its peroxy radicals can bind to lipids or proteins, or abstract a hydrogen atom from an unsaturated lipid, thereby causing lipid peroxidation and liver injury [41]. CCl_4 consistently induces liver damage in various animal species, even including non-human primates [42]. In previous studies, the activities of ALT, AST, as well as the levels of ALB, TBIL were abnormal [43], liver fibrosis was aggravated [44], the expressions of hepatocyte-specific markers (ALB, CK-18 and HNF4α) were decreased [45, 46], while the expressions of hepatic fibrosis-related proteins (α-SMA and collagen I) were increased in CCl_4-induced liver injury animal model [47], which were similar to the clinical symptoms of patients with liver injury [48, 49]. As expected, in the presented study, mice with CCl_4-induced liver injury exhibited abnormal serum liver function indexes, injured liver tissues as well as altered hepatocyte-specific marker expressions in the liver, suggesting the successful modeling of liver injury.

Exosomes play a pivotal role in MSCs-mediated repair of injured tissues. It has been demonstrated that CCl_4-induced liver injury can be alleviated by treatment with MSCs-derived exosomes [50, 51]. Interestingly, the therapeutic effects of MSCs depend entirely or partially on HGF secretion, and HGF-modified MSCs can enhance the therapeutic effects of MSCs [52]. The hepatoprotective effects of HGF have been widely reported. Following liver injury, HGF expression will be enhanced reactively to improve cellular regeneration [53]. A published study has demonstrated that HGF can protect the liver from radiation-induced injury by inhibiting apoptosis and transforming growth factor-β1 expression [54]. Moreover, an *in vivo* study has proved that HGF can reduce liver fibrosis for liver disease [55]. Shams *et al*. compared the effects of MSCs pretreated with HGF and untreated MSCs on CCl_4-induced hepatocytes, and found that the former provided better protection for CCl_4-induced hepatocytes than the latter, indicating the importance of overexpression of HGF for liver injury

repair and liver function recovery [56]. Consistently, in this study, we found that ADMSC-Exo can improve CCl_4-induced liver injury, and HGF magnified the effect of ADMSCs.

Later, we focused on the regulation of Rho GTPase by ADMSC^{HGF}-Exo. CDC42 and Rac1 belong to Rho GTPase protein family, the former regulates cell polarity, and the latter regulates the protrusion of lamellipodia at the leading edge [57]. More importantly, CDC42 and Rac1 can influence the downstream signal transduction pathway to promote the development of liver injury. Zheng *et al*. reported that miR-31 alleviated acetaminophen-induced liver injury by inhibiting CDC42 from limiting JNK signal over-activation [58]. Chaker *et al*. pointed out that inhibiting CDC42 through the Wnt5a/PI3K/miR-122 pathway enhanced the differentiation of ADMSCs-derived hepatocytes [59]. Zhao *et al*. found that abnormal activation of Rac1/JNK promoted CCl_4-induced liver injury [60]. Consistently, we also observed the high expressions of CDC42 and Rac1 in the liver tissues of model mice. In this study, we also discovered that ADMSC^{HGF}-Exo can effectively reduce the expressions of CDC42 and Rac1, indicating that ADMSC^{HGF}-Exo may alleviate liver injury by regulating Rho GTPase.

In a word, this study demonstrated that ADMSC^{HGF}--Exo exerted its hepatoprotective effects by regulating Rho GTPase, thereby alleviating liver fibrosis and restoring liver function in CCl_4-induced liver injury mice. This study hopes to provide an in-depth theoretical basis for the clinical application of ADMSC-Exo in liver injury.

Article information

Data availability statement

Data will be provided upon request.

Ethics statement

All procedures involving animals were approved by Ethic Committee of Zhejiang Eyong pharmaceutical research & development co., ltd (Certificate No. SYXK (Zhe) 2021-0033, Hangzhou, China).

Author contributions

Hanyu Zhou designed this study; JunChao Xue collected data; Yanyan Wu analyzed data; Liushenyan Yu drafted manuscript. Hanyu Zhou reviewed manuscript and all author read and approved the manuscript.

Funding

The authors declare that there were no funding.

Conflict of interest

The authors declare that there is no conflict of interest.

References

1. Lin F, Chen W, Zhou J, et al. Mesenchymal stem cells protect against ferroptosis via exosome-mediated stabilization of SLC7A11 in acute liver injury. Cell Death Dis. 2022; 13(3): 271, doi: 10.1038/s41419-022-04708-w, indexed in Pubmed: 35347117.
2. Peng C, Zhou Zm, Li J, et al. CCl_4-induced liver injury was ameliorated by Qi-Ge decoction through the antioxidant pathway. Evidence-Based Complementary and Alternative Medicine. 2019; 2019: 1–12, doi: 10.1155/2019/5941263.
3. Yang X, Jin Z, Lin D, et al. FGF21 alleviates acute liver injury by inducing the SIRT1-autophagy signalling pathway. J Cell Mol Med. 2022; 26(3): 868–879, doi: 10.1111/jcmm.17144, indexed in Pubmed: 34984826.
4. Hu C, Wu Z, Li L. Mesenchymal stromal cells promote liver regeneration through regulation of immune cells. Int J Biol Sci. 2020; 16(5): 893–903, doi: 10.7150/ijbs.39725, indexed in Pubmed: 32071558.
5. Solodeev I, Meilik B, Volovitz I, et al. Fas-L promotes the stem cell potency of adipose-derived mesenchymal cells. Cell Death Dis. 2018; 9(6): 695, doi: 10.1038/s41419-018-0702-y, indexed in Pubmed: 29891848.
6. Liu H, Wei LK, Jian XF, et al. Isolation, culture and induced differentiation of rabbit mesenchymal stem cells into osteoblasts. Exp Ther Med. 2018; 15(4): 3715–3724, doi: 10.3892/etm.2018.5894, indexed in Pubmed: 29581732.
7. Schmal H, Kowal JM, Kassem M, et al. Comparison of regenerative tissue quality following matrix-associated cell implantation using amplified chondrocytes compared to synovium-derived stem cells in a rabbit model for cartilage lesions. Stem Cells Int. 2018; 2018: 4142031, doi: 10.1155/2018/4142031, indexed in Pubmed: 29765410.
8. Mikłosz A, Nikitiuk BE, Chabowski A. Using adipose-derived mesenchymal stem cells to fight the metabolic complications of obesity: Where do we stand? Obes Rev. 2022; 23(5): e13413, doi: 10.1111/obr.13413, indexed in Pubmed: 34985174.
9. Vij R, Stebbings KA, Kim H, et al. Safety and efficacy of autologous, adipose-derived mesenchymal stem cells in patients with rheumatoid arthritis: a phase I/IIa, open-label, non-randomized pilot trial. Stem Cell Res Ther. 2022; 13(1): 88, doi: 10.1186/s13287-022-02763-w, indexed in Pubmed: 35241141.
10. Chang CL, Chen CH, Chiang JY, et al. Synergistic effect of combined melatonin and adipose-derived mesenchymal stem cell (ADMSC)-derived exosomes on amelioration of dextran sulfate sodium (DSS)-induced acute colitis. Am J Transl Res. 2019; 11(5): 2706–2724, indexed in Pubmed: 31217848.
11. Dong X, Shen LH, Yi Z, et al. Exosomes from adipose-derived stem cells can prevent medication-related osteonecrosis of the jaw. Med Sci Monit. 2021; 27: e929684, doi: 10.12659/MSM.929684, indexed in Pubmed: 33690263.
12. Fang Y, Zhang Y, Zhou J, et al. Adipose-derived mesenchymal stem cell exosomes: a novel pathway for tissues repair. Cell Tissue Bank. 2019; 20(2): 153–161, doi: 10.1007/s10561-019-09761-y, indexed in Pubmed: 30852701.
13. Doyle LM, Wang MZ. Overview of extracellular vesicles, their origin, composition, purpose, and methods for exosome isolation and analysis. Cells. 2019; 8(7), doi: 10.3390/cells8070727, indexed in Pubmed: 31311206.
14. Peng L, Chen Yu, Shi S, et al. Stem cell-derived and circulating exosomal microRNAs as new potential tools for diabetic nephropathy management. Stem Cell Res Ther. 2022;

13(1): 25, doi: 10.1186/s13287-021-02696-w, indexed in Pubmed: 35073973.
15. Gao Z, Han X, Zhu Y, et al. Drug-resistant cancer cell-derived exosomal EphA2 promotes breast cancer metastasis via the EphA2-Ephrin A1 reverse signaling. Cell Death Dis. 2021; 12(5): 414, doi: 10.1038/s41419-021-03692-x, indexed in Pubmed: 33879771.
16. Wang X, Liu D, Zhang X, et al. Exosomes from adipose-derived mesenchymal stem cells alleviate sepsis-induced lung injury in mice by inhibiting the secretion of IL-27 in macrophages. Cell Death Discov. 2022; 8(1): 18, doi: 10.1038/s41420-021-00785-6, indexed in Pubmed: 35013123.
17. Huang C, Zheng Y, Bai J, et al. Hepatocyte growth factor overexpression promotes osteoclastogenesis and exacerbates bone loss in CIA mice. J Orthop Translat. 2021; 27: 9–16, doi: 10.1016/j.jot.2020.10.011, indexed in Pubmed: 33344167.
18. Zhao Y, Ye W, Wang YD, et al. HGF/c-Met: a key promoter in liver regeneration. Front Pharmacol. 2022; 13: 808855, doi: 10.3389/fphar.2022.808855, indexed in Pubmed: 35370682.
19. Cheng W, Liu GP, Kong D, et al. Downregulation of miR-1224 protects against oxidative stress-induced acute liver injury by regulating hepatocyte growth factor. J Cell Biochem. 2019; 120(8): 12369–12375, doi: 10.1002/jcb.28502, indexed in Pubmed: 30848506.
20. Kaido T, Yamaoka S, Tanaka J, et al. Continuous HGF supply from HGF-expressing fibroblasts transplanted into spleen prevents CCl4-induced acute liver injury in rats. Biochem Biophys Res Commun. 1996; 218(1): 1–5, doi: 10.1006/bbrc.1996.0001, indexed in Pubmed: 8573112.
21. Dong Xi, Luo Y, Lu S, et al. Ursodesoxycholic acid alleviates liver fibrosis via proregeneration by activation of the ID1-WNT2/HGF signaling pathway. Clin Transl Med. 2021; 11(2): e296, doi: 10.1002/ctm2.296, indexed in Pubmed: 33635004.
22. Rizvi F, Everton E, Smith AR, et al. Murine liver repair via transient activation of regenerative pathways in hepatocytes using lipid nanoparticle-complexed nucleoside-modified mRNA. Nat Commun. 2021; 12(1): 613, doi: 10.1038/s41467-021-20903-3, indexed in Pubmed: 33504774.
23. Cao T, Xiao D, Ji P, et al. [Effects of exosomes from hepatocyte growth factor-modified human adipose mesenchymal stem cells on full-thickness skin defect in diabetic mice]. Zhonghua Shao Shang Za Zhi. 2022; 38(11): 1004–1013, doi: 10.3760/cma.j.cn501225-20220731-00330, indexed in Pubmed: 36418257.
24. Ghoreshi ZA, Kabirifar R, Khodarahmi A, et al. The preventive effect of atorvastatin on liver fibrosis in the bile duct ligation rats via antioxidant activity and down-regulation of Rac1 and NOX1. Iran J Basic Med Sci. 2020; 23(1): 30–35, doi: 10.22038/IJBMS.2019.33663.8047, indexed in Pubmed: 32395205.
25. Wang R, Wang X, Zhuang L. Gene expression profiling reveals key genes and pathways related to the development of non-alcoholic fatty liver disease. Ann Hepatol. 2016; 15(2): 190–199, doi: 10.5604/16652681.1193709, indexed in Pubmed: 26845596.
26. Wang DS, Dou KF, Li KZ, et al. Enhancement of migration and invasion of hepatoma cells via a Rho GTPase signaling pathway. World J Gastroenterol. 2004; 10(2): 299–302, doi: 10.3748/wjg.v10.i2.299, indexed in Pubmed: 14716844.
27. Wells CM, Ahmed T, Masters JRW, et al. Rho family GTPases are activated during HGF-stimulated prostate cancer-cell scattering. Cell Motil Cytoskeleton. 2005; 62(3): 180–194, doi: 10.1002/cm.20095, indexed in Pubmed: 16211585.
28. Cao Y, Tan J, Zhao H, et al. Bead-jet printing enabled sparse mesenchymal stem cell patterning augments skeletal muscle and hair follicle regeneration. Nat Commun. 2022; 13(7463), doi: 10.1038/s41467-022-35183-8.
29. Zhang Y, Yu X, Wang Z, et al. Pokeweed antiviral protein attenuates liver fibrosis in mice through regulating Wnt/Jnk mediated glucose metabolism. Saudi J Gastroenterol. 2018; 24(3): 157–164, doi: 10.4103/sjg.SJG_470_17, indexed in Pubmed: 29652027.
30. Liu M, Jia H, He Y, et al. Preventive effects of aqueous extract on high-fat diet-induced fatty liver of mice. Evid Based Complement Alternat Med. 2022; 2022: 7183471, doi: 10.1155/2022/7183471, indexed in Pubmed: 35432557.
31. Heindryckx F, Binet F, Ponticos M, et al. Endoplasmic reticulum stress enhances fibrosis through IRE1α-mediated degradation of miR-150 and XBP-1 splicing. EMBO Mol Med. 2016; 8(7): 729–744, doi: 10.15252/emmm.201505925, indexed in Pubmed: 27226027.
32. Zhang J, Zhou S, Zhou Yi, et al. Hepatocyte growth factor gene-modified adipose-derived mesenchymal stem cells ameliorate radiation induced liver damage in a rat model. PLoS One. 2014; 9(12): e114670, doi: 10.1371/journal.pone.0114670, indexed in Pubmed: 25501583.
33. Hu C, Zhao L, Zhang L, et al. Mesenchymal stem cell-based cell-free strategies: safe and effective treatments for liver injury. Stem Cell Res Ther. 2020; 11(1): 377, doi: 10.1186/s13287-020-01895-1, indexed in Pubmed: 32883343.
34. Chang YJ, Liu JW, Lin PC, et al. Mesenchymal stem cells facilitate recovery from chemically induced liver damage and decrease liver fibrosis. Life Sci. 2009; 85(13-14): 517–525, doi: 10.1016/j.lfs.2009.08.003, indexed in Pubmed: 19686763.
35. Couto BG, Goldenberg RC, da Fonseca LMB, et al. Bone marrow mononuclear cell therapy for patients with cirrhosis: a phase 1 study. Liver Int. 2011; 31(3): 391–400, doi: 10.1111/j.1478-3231.2010.02424.x, indexed in Pubmed: 21281433.
36. Spahr L, Chalandon Y, Terraz S, et al. Autologous bone marrow mononuclear cell transplantation in patients with decompensated alcoholic liver disease: a randomized controlled trial. PLoS One. 2013; 8(1): e53719, doi: 10.1371/journal.pone.0053719, indexed in Pubmed: 23341981.
37. Satilmis B, Cicek GS, Cicek E, et al. Adipose-derived stem cells in the treatment of hepatobiliary diseases and sepsis. World J Clin Cases. 2022; 10(14): 4348–4356, doi: 10.12998/wjcc.v10.i14.4348, indexed in Pubmed: 35663078.
38. Deng L, Liu G, Wu X, et al. Adipose derived mesenchymal stem cells efficiently rescue carbon tetrachloride-induced acute liver failure in mouse. ScientificWorldJournal. 2014; 2014: 103643, doi: 10.1155/2014/103643, indexed in Pubmed: 24999489.
39. Salunkhe S, Basak M, Chitkara D, et al. Surface functionalization of exosomes for target-specific delivery and in vivo imaging & tracking: Strategies and significance. J Control Release. 2020; 326: 599–614, doi: 10.1016/j.jconrel.2020.07.042, indexed in Pubmed: 32730952.
40. Zheng Y, Cui B, Sun W, et al. Potential crosstalk between liver and extra-liver organs in mouse models of acute liver injury. Int J Biol Sci. 2020; 16(7): 1166–1179, doi: 10.7150/ijbs.41293, indexed in Pubmed: 32174792.
41. Adetoro KO, Bolanle JD, Abdullahi SB, et al. In vivo antioxidant effect of aqueous root bark, stem bark and leaves extracts of Vitex doniana in CCl4 induced liver damage rats. Asian Pac J Trop Biomed. 2013; 3(5): 395–400, doi: 10.1016/S2221-1691(13)60083-0, indexed in Pubmed: 23646304.
42. Yoshida T, Adachi E, Nigi H, et al. Changes of sinusoidal basement membrane collagens in early hepatic fibrosis induced with CCl4 in cynomolgus monkeys. Pathology. 1999; 31(1): 29–35, doi: 10.1080/003130299105494, indexed in Pubmed: 10212919.
43. Chen Mi, Wang T, Jiang ZZ, et al. Anti-inflammatory and hepatoprotective effects of total flavonoid C-glycosides from Abrus mollis extracts. Chin J Nat Med. 2014; 12(8): 590–

598, doi: 10.1016/S1875-5364(14)60090-X, indexed in Pubmed: 25156284.
44. Liu L, Guo H, Shao C, et al. Shugan Huoxue Huayu Fang attenuates carbon tetrachloride-induced hepatic fibrosis in rats by inhibiting transforming growth factor-β1/Smad signaling. J Tradit Chin Med. 2022; 42(1): 65–72, doi: 10.19852/j.cnki.jtcm.20210624.001, indexed in Pubmed: 35294124.
45. Idriss NK, Sayyed HG, Osama A, et al. Treatment efficiency of different routes of bone marrow-derived mesenchymal stem cell injection in rat liver fibrosis model. Cell Physiol Biochem. 2018; 48(5): 2161–2171, doi: 10.1159/000492558, indexed in Pubmed: 30114694.
46. Liu Q, Lei X, Cao Z, et al. TRPM8 deficiency attenuates liver fibrosis through S100A9-HNF4α signaling. Cell Biosci. 2022; 12(1): 58, doi: 10.1186/s13578-022-00789-4, indexed in Pubmed: 35525986.
47. Shrestha N, Chand L, Han MK, et al. Glutamine inhibits CCl4 induced liver fibrosis in mice and TGF-β1 mediated epithelial-mesenchymal transition in mouse hepatocytes. Food Chem Toxicol. 2016; 93: 129–137, doi: 10.1016/j.fct.2016.04.024, indexed in Pubmed: 27137983.
48. Zhu Y, Niu M, Wang JB, et al. Predictors of poor outcomes in 488 patients with herb-induced liver injury. Turk J Gastroenterol. 2019; 30(1): 47–58, doi: 10.5152/tjg.2018.17847, indexed in Pubmed: 30289391.
49. Chijioke O, Bawohl M, Springer E, et al. Hepatitis e virus detection in liver tissue from patients with suspected drug-induced liver injury. Front Med (Lausanne). 2015; 2: 20, doi: 10.3389/fmed.2015.00020, indexed in Pubmed: 25870858.
50. Sabry D, Mohamed A, Monir M, et al. The effect of mesenchymal stem cells derived microvesicles on the treatment of experimental CCL4 induced liver fibrosis in rats. Int J Stem Cells. 2019; 12(3): 400–409, doi: 10.15283/ijsc18143, indexed in Pubmed: 31474025.
51. Gupta S, Sharma H, Soni N, et al. Comparative evaluation of anti-fibrotic effect of tissue specific mesenchymal stem cells derived extracellular vesicles for the amelioration of ccl4 induced chronic liver injury. Stem Cell Rev Rep. 2022; 18(3): 1097–1112, doi: 10.1007/s12015-021-10313-9, indexed in Pubmed: 34859376.
52. Meng HF, Jin J, Wang H, et al. Recent advances in the therapeutic efficacy of hepatocyte growth factor gene-modified mesenchymal stem cells in multiple disease settings. J Cell Mol Med. 2022; 26(18): 4745–4755, doi: 10.1111/jcmm.17497, indexed in Pubmed: 35922965.
53. McElroy AK, Harmon JR, Flietstra T, et al. Human biomarkers of outcome following rift valley fever virus infection. J Infect Dis. 2018; 218(11): 1847–1851, doi: 10.1093/infdis/jiy393, indexed in Pubmed: 29955891.
54. Chi CH, Liu IL, Lo WY, et al. Hepatocyte growth factor gene therapy prevents radiation-induced liver damage. World J Gastroenterol. 2005; 11(10): 1496–1502, doi: 10.3748/wjg.v11.i10.1496, indexed in Pubmed: 15770726.
55. Jiang Zz, Xia Gy, Zhang Y, et al. Attenuation of hepatic fibrosis through ultrasound-microbubble-mediated HGF gene transfer in rats. Clin Imaging. 2013; 37(1): 104–110, doi: 10.1016/j.clinimag.2012.02.017, indexed in Pubmed: 23206615.
56. Shams S, Mohsin S, Nasir GA, et al. Mesenchymal stem cells and Interleukin-6 attenuate liver fibrosis in mice. J Transl Med. 2013; 11: 78, doi: 10.1186/1479-5876-11-78, indexed in Pubmed: 23531302.
57. Mosaddeghzadeh N, Ahmadian MR. The RHO family GTPases: mechanisms of regulation and signaling. Cells. 2021; 10(7), doi: 10.3390/cells10071831, indexed in Pubmed: 34359999.
58. Zheng J, Zhou H, Yang T, et al. Protective role of microRNA-31 in acetaminophen-induced liver injury: a negative regulator of c-Jun N-terminal kinase (JNK) signaling pathway. Cell Mol Gastroenterol Hepatol. 2021; 12(5): 1789–1807, doi: 10.1016/j.jcmgh.2021.07.011, indexed in Pubmed: 34311140.
59. Chaker D, Mouawad C, Azar A, et al. Inhibition of the RhoGTPase Cdc42 by ML141 enhances hepatocyte differentiation from human adipose-derived mesenchymal stem cells via the Wnt5a/PI3K/miR-122 pathway: impact of the age of the donor. Stem Cell Res Ther. 2018; 9(1): 167, doi: 10.1186/s13287-018-0910-5, indexed in Pubmed: 29921325.
60. Zhao X, Fu J, Xu A, et al. Gankyrin drives malignant transformation of chronic liver damage-mediated fibrosis via the Rac1/JNK pathway. Cell Death Dis. 2015; 6(5): e1751, doi: 10.1038/cddis.2015.120, indexed in Pubmed: 25950481.

Submited: 25 April, 2023
Accepted after reviews: 21 September, 2023
Available as AoP: 3 October, 2023